Polymer Journal, Vol. 39, No. 12, pp. 1290–1294 (2007)

SPECIAL ISSUES -PROGRESS IN STRUCTURE ANALYSES OF POLYMERIC MATERIALS BY SYNCHROTRON RADIATION AND NEUTRON BEAM-

Gas Sorption into Surface of Poly(methyl methacrylate) Films at Atmospheric Pressure

Yoshihisa FUJII,[1] Hironori ATARASHI,[1] Norifumi YAMADA,[2] Naoya TORIKAI,[2] Toshihiko NAGAMURA,[1,†] and Keiji TANAKA[1,†]

[1]*Department of Applied Chemistry, Faculty of Engineering, Kyushu University, 744 Motooka, Nishi-ku, Fukuoka 819-0395, Japan*
[2]*Neutron Science Laboratory, High Energy Accelerator Research Organization, 1-1 Oho, Tsukuba 305-0801, Japan*

(Received June 6, 2007; Accepted September 4, 2007; Published October 16, 2007)

ABSTRACT: Interfacial structure of deuterated poly(methyl methacrylate) (dPMMA) and polystyrene (dPS) films with gases such as carbon dioxide (CO_2) and nitrogen (N_2) under a pressure of 0.1 MPa was examined by neutron reflectivity (NR). The interface was analyzed using a model that the density of the outermost region of the films was lower than that of the interior region. The density profile was expressed by a single exponential equation with a decay length (ξ). The ξ values for the dPMMA films under CO_2 and N_2 were larger than that under vacuum at a given temperature, and the extent was more remarkable under CO_2 than under N_2. On the other hand, such a gas sorption was not clearly discerned for the dPS films. Finally, the surface relaxation in the dPMMA and dPS films under CO_2 and N_2 was discussed on the basis of lateral force measurements. [doi:10.1295/polymj.PJ2007070]

KEY WORDS Neutron Reflectivity / Interface / Density Profiles / Poly(methyl methacrylate) / Polystyrene /

Physical properties of polymers at surfaces and interfaces often differ from those in the corresponding bulk ones. In the last two decades, it has been extensively studied, experimentally and theoretically, how and why the presence of surface and interface must alter inherent properties of polymers.[1–4] Such studies are quite important in the fields of photolithography, protective coatings, lubricants, adhesives, permselective membranes, biomaterials, etc, because the surface and interfacial layers with specific structure and physical properties play crucial roles in the applications. When polymer materials are used for the aforementioned applications, the surface is supposed to be contacted with other phases in reality. That is, the surface serves as the interface. Therefore, structure and dynamics at the polymer interfaces should be studied after understanding surface structure and properties.

Polymers are often used as key materials for gas separation membranes due to their superior permeability-selectivity balance. In this case, interactions between polymer surface and gas molecules should be understood at first so that the functionality is promisingly improved. While such studies have been widely made at high pressures,[5–9] this is not the case under a gentle condition like at an atmospheric pressure. However, to address clearly the interaction, it should be studied what happens if gas molecules contact with the polymer surface at an ambient atmosphere.

In this study, we chose typical glassy polymers such as poly(methyl methacrylate) (PMMA) and polystyrene (PS), which have been used in a wide variety of technological applications. Then, aggregation states of the polymers at the interfaces with gases such as carbon dioxide (CO_2) and nitrogen (N_2) were examined by neutron reflectivity (NR) with a temperature cell. Based on NR measurement, we gain an access to the density profile of polymers along the direction normal to the surface as well as the film thickness with the depth resolution better than 1 nm.[10–13] When gas molecules are sorbed in the polymers, the physical properties should be concurrently altered. Hence, lateral force of the polymers, reflecting the viscoelastic response at the outermost region, was also examined under the presence of those gases.

EXPERIMENTAL

Monodisperse and perdeuterated PMMA (dPMMA) and PS (dPS) were purchased from Polymer Source Inc. The number-average molecular weight of dPMMA and dPS were 296 k and 317 k, respectively. The bulk glass transition temperature (T_g^b), which

†To whom correspondence should be addressed (Tel: +81-92-802-2879, Fax: +81-92-802-2880, E-mail: k-tanaka@cstf.kyushu-u.ac.jp).

Table I. Scattering length density (b/V) values for polymers and gases used in this study

	$(b/V)/\mathrm{nm}^{-2}$
dPMMA	6.62×10^{-4}
dPS	6.22×10^{-4}
CO_2	4.91×10^{-7}
N_2	5.03×10^{-7}

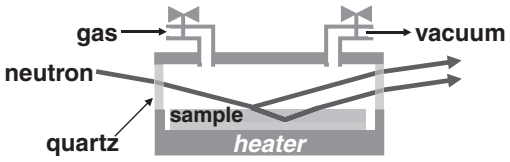

Figure 1. Schematic illustration of experimental set-up for NR measurement.

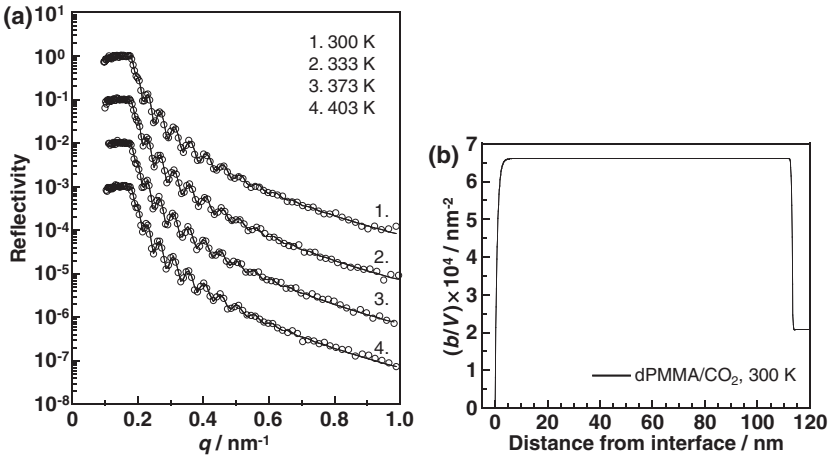

Figure 2. (a) Neutron reflectivity for a dPMMA film under CO_2 atmosphere of 0.1 MPa at 300, 333, 373 and 403 K. Circles are experimental data, and solid lines depict reflectivity calculated on the basis of model scattering length density profiles. The data is offset by a decade for clarity. (b) A typical model scattering length density profile for a (dPMMA/CO_2) system at 300 K.

was determined by differential scanning calorimetry (DSC220, SII NanoTechnology Inc.) at the heating rate of $10\,\mathrm{K\cdot min^{-1}}$ under dry nitrogen purge, was 399 and 377 K, respectively. Polymer films were spin-coated from each toluene solution onto Si substrates with a native oxide layer. They were dried under the ambient atmosphere at room temperature for more than 24 h, and then, annealed under vacuum at 423 K for 24 h. The film thickness after the drying process was evaluated to be 110 nm by ellipsometry (M-150, JASCO Co., Ltd.). As gases, CO_2 and N_2 were used. This was because they were regarded as gases with and without a good affinity to PMMA, respectively. Table I shows the scattering length density (b/V) values for polymers and gases used in this study. NR measurement was performed using the advanced reflectometer for interface and surface analysis (ARISA)[14] on the H5 beamline of the Neutron Science Laboratory, High Energy Accelerator Research Organization. Figure 1 shows the schematic illustration of the experimental set-up in a gas atmosphere. The neutron beam was transmitted through a series of quartz windows in the temperature cell. The gas pressure was regulated to be 0.1 MPa, corresponding to the atmospheric pressure. The NR data were plotted versus the scattering vector (q) which was defined by $(4\pi/\lambda)\cdot\sin\theta$, where λ and θ were wavelength and incident angle of the neutron beam, respectively. The incident neutrons wavelength band was 0.05–0.4 nm. The reflectivity was calculated on the basis of the (b/V) profile along the depth direction using Parratt32, which was a freeware from the Hahn-Meitner Institute (HMI).[15]

Viscoelastic response at the outermost region of the dPMMA and dPS films was examined under the presence of CO_2 and N_2 by lateral force microscopy (LFM, SPA300HV, SII NanoTechnology Inc.) with an SPI3800 controller. The spring constant of cantilevers used was estimated to be *ca.* $0.1\,\mathrm{N\cdot m^{-1}}$ and the tip radius of curvature was typically less than 20 nm. The normal force onto the cantilevers was set to be approximately 10 nN.

RESULTS AND DISCUSSION

Figure 2(a) shows the scattering vector dependence of reflectivity for dPMMA films under CO_2 atmosphere at 300, 333, 373 and 403 K. The data at 333, 373 and 403 K are offset by a decade for the sake of clarity. Solid lines denote the best-fit calculated reflectivity, to the experimental data, on the basis of model scattering length density (b/V) profiles. A typical example of (b/V) profile and fitting parameters are shown in the panel (b) of

Table II. Fitting parameters for a (dPMMA/CO_2) system at 300 K

	dPMMA/CO_2
film thickness/nm	113.1
roughness/nm	0.51
ξ/nm	7.70
χ^2	9.72×10^{-3}

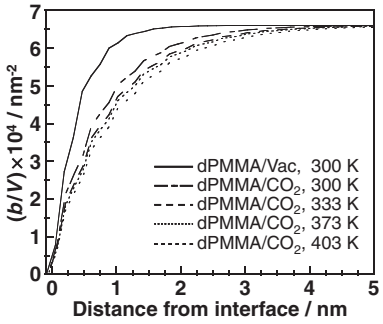

Figure 3. Enlarged model (b/V) profiles, in the depth range of 5 nm, for a (dPMMA/CO_2) system at 300, 333, 373 and 403 K.

Figure 2 and Table II, respectively. Since the calculated curves are in good agreement with the experimental data, it can be claimed that the model (b/V) profiles used well reflect the density profiles of the dPMMA film along the direction normal to the interface.

Figure 3 shows the enlarged model (b/V) profiles for the (dPMMA/CO_2) system at 300, 333, 373 and 403 K. The (b/V) value asymptotically reached a constant at the depth of approximately 5 nm for all the cases, although the (b/V) depletion was more prominent at a higher temperature. Since the (b/V) values for dPMMA and CO_2 were 6.62×10^{-4} and 4.91×10^{-7} nm^{-2}, respectively, it seems most likely that a decrease in the (b/V) value corresponds to a reduction of the density and/or an increase in the CO_2 fraction in the vicinity of the interface. Here, two points should be emphasized. First, the (b/V) in the interfacial region was lower under CO_2 than under vacuum at

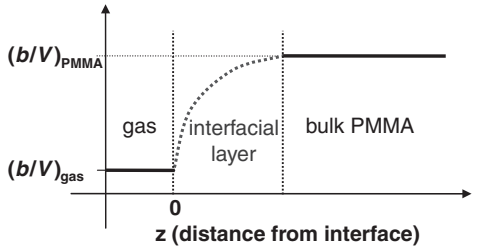

Figure 4. Schematic illustration of model scattering length density profile for a dPMMA film under gas atmosphere.

300 K. In general, the density of a polymer in the surface region under the presence of a gas at 0.1 MPa should be higher than that under vacuum.[16] Nevertheless, the opposite was observed by our experiments. Thus, we may have to think that CO_2 molecules penetrate into the outermost region of the dPMMA film even at a pressure of 0.1 MPa. Second, under CO_2, the (b/V) depletion became more remarkable with increasing temperature. This point will be discussed after Figure 5.

We here take a model that the density of the outermost region of the films was lower than that of the interior region. This density reduction was supposed to be emphasized by the gas penetration, as mentioned above. Figure 4 illustrates the model which can be expressed by a single exponential equation with the decay length (ξ). Thus, the (b/V) value at a depth of z is given by

$$(b/V) = \{(b/V)_{dPMMA} - (b/V)_{gas}\} \cdot \{1 - \exp(-z/\xi)\} + (b/V)_{gas}$$

The panels (a) and (b) of Figure 5 show the temperature dependence of ξ for the dPMMA and dPS films under three different environments. As a general trend, the ξ value increased with increasing temperature. In the case of the dPMMA films, the ξ values under CO_2 and N_2 atmospheres were larger than that under vacuum at a given temperature, meaning that the gas molecules penetrated into the outermost region of the film. It is worthy to note that this was the case

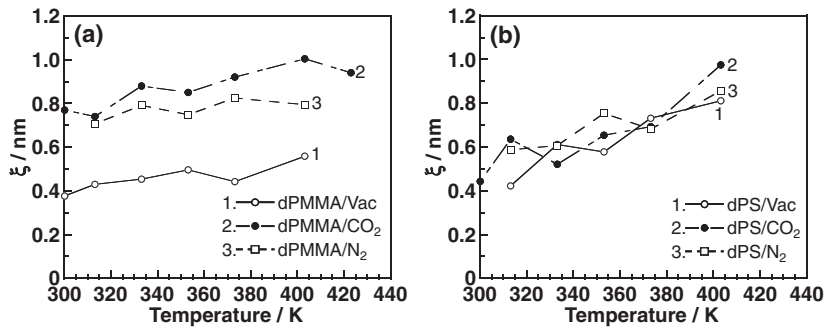

Figure 5. Temperature dependence of decay length (ξ) for (a) dPMMA and (b) dPS films.

Table III. Gas solubility to PMMA and PS

	solubility $\times 10^3 / \frac{cm^3(STP)}{cm^3 cmHg}$	
	CO_2	N_2
PMMA	53.2	1.79
PS	0.33	0.025

even for N_2, which had been regarded as an inert gas. The extent of the gas sorption was more striking under CO_2 than under N_2. On the other hand, a clear dependence of ξ on the environment was not observed for the dPS films, as shown in the panel (b) of Figure 5. In addition, the ξ value for the dPS films was smaller than that for the dPMMA films at a given temperature up to $T_g{}^b$ of the PS. These results might be related to the gas solubility into the polymers, as shown in Table III.[17]

Here, it is discussed why CO_2 exhibits a good affinity to dPMMA. Eckert and co-workers have studied, using Fourier transform infrared (FT/IR) spectroscopy, an interaction of CO_2 with polymers.[18–20] They have concluded that polymers containing carbonyl groups would act as an electron donor, and that a specific intermolecular interaction between the polymer and CO_2, which behaves as an electron acceptor rather than as an electron donor, is attained.[20] Although a weak electrostatic interaction[21] is possible to a pair of CO_2 and phenyl π-electrons of PS, PS does not show a strong interaction with CO_2 owing to a lack of carbonyl groups. These arguments are consistent with what is seen in Figure 5.

However, the temperature dependence of ξ is not so simple to be fully understood. This is because the phenomenon is controlled by not only gas solubility but also thermal molecular motion, or density. The ξ value increased with increasing temperature even under vacuum for both dPS and dPMMA. This means that the interfacial layer in which the density is reduced, or the mobility is enhanced, thickens with increasing temperature. This notion is in good accordance with our previous publications.[10,22] Then, the slope of the plot in Figure 5 is discussed. In the case of dPS, the surface glass transition temperature ($T_g{}^s$) and $T_g{}^b$ were roughly 340 and 380 K, respectively. These values for dPMMA should be, respectively, 320 and 400 K. Thus, the temperature employed for the measurement ranged from far below the $T_g{}^s$ to above the $T_g{}^b$ for dPS. On the contrary, in the case of dPMMA, the temperature region employed was almost comparable to the range being from the $T_g{}^s$ to the $T_g{}^b$. These should be correlated to why the slope of the plot in Figure 5 was larger for dPS than dPMMA.

The solubility of a gas into a polymer generally decreases with increasing temperature.[23] Nevertheless, the ξ here increased with increasing temperature, as shown in Figure 5. Moreover, to what extent gas molecules were sorbed into polymers was not necessarily consistent with the solubility difference. Thus, it is plausible that the gas sorption into the film surface is quite complicated at a gentle pressure like 0.1 MPa and is controlled by not a single factor of the gas solubility but a few or many factors. One candidate for those is thermal molecular motion of the polymers, as discused. But, further study is necessary to conclude which factor is the most crucial on the gas penetration into the polymers, especially the surface region, under such a gentle pressure.

When gas molecules are sorbed into the polymers, physical properties of the polymers should be altered. Hence, lateral force for the dPMMA and dPS films, reflecting viscoelastic response at the outermost region, was also examined under the presence of CO_2 and N_2. Figure 6 shows the typical lateral force curves for the dPMMA and dPS films at 333 K under CO_2 and N_2 atmospheres. Upper and lower parts in a lateral force loop correspond to the extent of the torsion for a cantilever during a tip sliding for back and forth on the film. Hence, the difference of upper and lower parts, namely trace and retrace, is proportional to the magnitude of lateral force. Lateral force curves in Figure 6 were normalized by using the one under the presence of N_2. In the case of dPMMA,

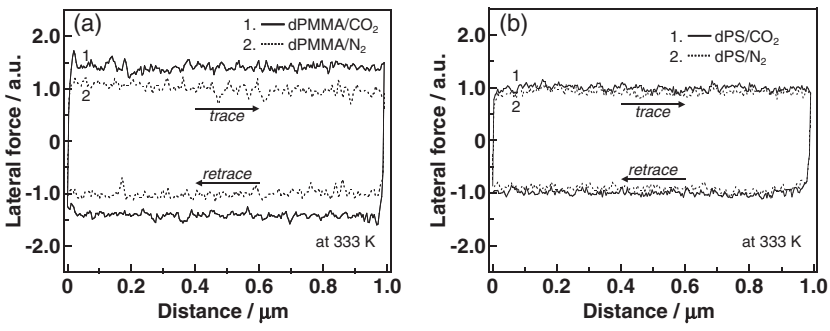

Figure 6. Lateral force curves for (a) dPMMA and (b) dPS films at 333 K.

the lateral force was larger under CO_2 than under N_2. On the other hand, the lateral force was not sensitive to the gas species for dPS. These results make it clear that the outermost region of the dPMMA film under CO_2 than N_2 differs each other in terms of viscoelastic properties.

Lateral force difference observed for the dPMMA film between CO_2 than N_2 might be interpreted by the difference of the interfacial layer thickness. Taking into account the ξ values under CO_2 and N_2, the tip penetration was more striking for CO_2 than for N_2 on account of the softness, under the condition of a given normal force onto the tip. In general, as a tip deeper penetrates into a polymer, the lateral force becomes larger. If that is the case, it was quite reasonable that the lateral forces for the dPS film under CO_2 and N_2 were comparable.

However, interpretation for lateral force observed for a polymer is actually not so simple. The lateral force for the polymer, being in a relaxation process, is larger than those being before and after the process. When gas molecules penetrated into the polymer films, the surface relaxation temperatures would be lowered from the original ones.[23] This means that the magnitude of lateral force is dominated by not only the tip penetration depth but also the lowering of the surface relaxation temperatures. Either way, systematic study is necessary to conclude the issue in the future.

CONCLUSIONS

It was shown that NR was a powerful tool to examine how gas molecules were sorbed into polymers on the nanometer level. CO_2 than N_2 gases could penetrate into the outermost region of the dPMMA films even at 0.1 MPa, being approximately the atmospheric pressure. However, the dependence of the density depletion layer on the environment was not clear for the dPS films. Surface relaxation behaviors for the dPMMA and dPS films under CO_2 and N_2 were in good accordance with the NR results. Although the gas sorption process was quite complicated, it seems most likely that the gas solubility and the molecular motion of polymers were responsible in what was seen in our experiments.

Acknowledgment. This research was in part supported by the Inter-Univ. Program for common use KEK-KENS, by Industrial Technology Research Grant Program in 2006 from New Energy and Industrial Technology Development Organization (NEDO) of Japan, and by the Grant-in-Aids for Young Scientists A (No. 18685014) and Science Research in a Priority Area "Soft Matter Physics" (No. 19031021) from the Ministry of Education, Culture, Sports, Science and Technology, Japan.

REFERENCES

1. I. Sanchez, in "Physics of Polymer Surfaces and Interfaces," Butterworth-Heinemann, Stoneham, 1992.
2. F. Garbassi, M. Morra, and E. Occhiello, in "Polymer Surfaces, from Physics to Technology," Wiley, Chichester, 1994.
3. R. A. L. Jones and R. W. Richards, in "Polymers at Surfaces and Interfaces," Cambridge University Press, Cambridge, 1999.
4. "Polymer Surfaces, Interfaces and Thin Films," A. Karim and S. Kumar, Ed., World Scientific, Singapore, 2000.
5. Y. T. Shieh and K. H. Liu, *J. Supercrit. Fluids*, **25**, 261 (2003).
6. T. Koga, Y. Ji, Y. S. Seo, C. Gordon, F. Qu, M. H. Rafailovich, J. C. Sokolov, and S. K. Satija, *J. Polym. Sci., Part B: Polym. Phys.*, **42**, 3282 (2004).
7. V. Carla, K. Wang, Y. Hussain, K. Efimenko, J. Genzer, C. Grant, G. C. Sarti, R. G. Carbonell, and F. Doghieri, *Macromolecules*, **38**, 10299 (2005).
8. O. S. Fleming, K. L. A. Chan, and S. G. Kazarian, *Polymer*, **47**, 4649 (2006).
9. M. Pantoula and C. Panayiotou, *J. Supercrit. Fluids*, **37**, 254 (2006).
10. D. Kawaguchi, K. Tanaka, T. Kajiyama, A. Takahara, and S. Tasaki, *Macromolecules*, **36**, 1235 (2003).
11. M. Harada, T. Suzuki, M. Ohya, D. Kawaguchi, A. Takano, Y. Matsushita, and N. Torika, *J. Polym. Sci., Part B: Polym. Phys.*, **43**, 1486 (2005).
12. A. Noro, M. Okuda, F. Odamaki, D. Kawaguchi, N. Torikai, A. Takano, and Y. Matsushita, *Macromolecules*, **39**, 7654 (2006).
13. M. Ujihara, K. Mitamura, N. Torikai, and T. Imae, *Langmuir*, **22**, 3656 (2006).
14. N. Torikai, M. Furusaka, H. Matsuoka, Y. Matsushita, M. Shibayama, A. Takahara, M. Takeda, S. Tasaki, and H. Yamaoka, *Appl. Phys. A: Mater. Sci. Process.*, **74**, S264 (2002).
15. http://www.hmi.de/bensc/instrumentation/instrumente/v6/refl/parratt_en.htm
16. J. Cho and I. C. Sanchez, in "Polymer Handbook," 4th ed., J. Brandrup, E. H. Immergut, and E. A Grulke, Ed., Wiley, New York, 1999, Vol. VI, pp 591.
17. K. E. Min and D. R. Paul, *J. Polym. Sci., Part B; Polym. Phys.*, **26**, 1021 (1988).
18. A. Higuchi and T. Nakagawa, *J. Polym. Sci., Part B: Polym. Phys.*, **32**, 149 (1994).
19. B. J. Briscoe and C. T. Kelly, *Polymer*, **36**, 3099 (1995).
20. S. G. Kazarian, M. F. Vincent, F. V. Bright, C. L. Liotta, and C. A. Eckert, *J. Am. Chem. Soc.*, **118**, 1729 (1996).
21. A. R. Manninen, H. E. Naguib, A. V. Nawaby, and M. Day, *Polym. Eng. Sci.*, **45**, 904 (2005).
22. Y. Tateishi, K. Tanaka, and T. Nagamura, *J. Phys. Chem. B*, **111**, 7761 (2007).
23. Y. Yang, M. M. Cheng, X. Hu, D. Liu, R. J. Goyette, L. J. Lee, and M. Ferrari, *Macromolecules*, **40**, 1108 (2007).